IEEE Access
Multidisciplinary ⋮ Rapid Review ⋮ Open Access Journal

Received April 3, 2021, accepted April 9, 2021, date of publication April 12, 2021, date of current version April 21, 2021.

Digital Object Identifier 10.1109/ACCESS.2021.3072777

Harmonic Beamforming Based on Modified Single-Sideband Time Modulated Phased Array and Its Enhanced Version

YUE MA, (Student Member, IEEE), CHEN MIAO, (Member, IEEE), YUE-HUA LI, (Member, IEEE), AND WEN WU, (Senior Member, IEEE)

Ministerial Key Laboratory of JGMT, School of Electronic Engineering and Optoelectronic Technology, Nanjing University of Science and Technology, Nanjing 210094, China

Corresponding author: Chen Miao (miaochen78@163.com)

This work was supported by the Science and Technology on Near-Surface Detection Laboratory under Grant 6142414200101.

ABSTRACT Recently, harmonic beamforming in the time-modulated array (TMA) has attracted much attention. In this study, two kinds of beamforming systems of TMA based on the single-sideband time-modulated phased array (STMPA) and enhanced STMPA are presented, and the $+1^{st}$ harmonic beamforming is performed. Based on the basic structure of STMPA and ESTMPA, we transform the design of the I/Q modulator, then the modified STMPA (MSTMPA) and modified ESTMPA (MESTMPA) are presented. The two channels in an I/Q modulator are each connected to an antenna with other structures keep constant. Hence, the number of antennas can be multiplied, and the system complexity can be reduced with an increase in the number of antennas especially for large-scale applications. In addition, the array aperture is enlarged with the same number of I/Q modulators, and the performance of the beam pattern is improved. However, without the single sideband structure, the $(4k-1 \cap 3k)^{st}$ and $(8k-1)^{st}$ harmonics in STMPA and ESTMPA cannot be eliminated; therefore, the bandpass filter is used at the output of the system; thus, the $+1^{st}$ harmonic can be extracted. The derivations and analysis are given in detail, and STMPA and ESTMPA compared. Finally, the effectiveness of the proposed systems is verified by simulation results and the $+1^{st}$ harmonic can be formed in desired directions.

INDEX TERMS Time-modulated array, single-sideband time modulated phased array, switching sequences, radio frequency switches, harmonic beamforming.

I. INTRODUCTION

Time-modulated array (TMA) was originally proposed in the 1960s [1]. Different from the phased array, TMA uses the radio frequency (RF) switches instead of the phase shifter, which can reduce the complexity of the system. By controlling switching sequences, ultralow sidelobe can be achieved. However, limited by the device performance, studies on this at the beginning of the century were few. With the development of the performance of RF switches, processors, filters, and other devices, TMA was realized in the 2000s [2]. Presently, studies on TMA are springing up. Several harmonics at different frequencies are generated because of the switching mode of TMA, and most of them are undesired for use. Thus, most researches focus on harmonic suppression [2]–[4]. Currently, optimization methods are used to obtain the switching sequences that can suppress the sideband level (SBL), such as particle swarm optimizer (PSO) [2], differential evolution (DE) [3], and genetic algorithm (GA) [5], [6], and they have proven to useful.

Meanwhile, the harmonics generated by TMA can achieve beam scanning and low sidelobe level (SLL). Several studies on harmonics [7]–[9] have sprung up. The array factor of harmonics generated by TMA can be calculated using the Fourier series; thus, it can be controlled by designing switching sequences. This indicates that harmonics are not harmful, since they can be properly controlled. The harmonic beamforming can be used in direction finding [10], [11], communications [12], [13], and radar [15].

The weighting control method of $+1^{st}$ harmonic in a time-modulated linear array was proposed in [7]. It provides a method to tune the modulation time of a single element to control the output of the entire array. However, the traditional TMA structure was not efficient. Subsequently, the

The associate editor coordinating the review of this manuscript and approving it for publication was Pavlos I. Lazaridis.

single-sideband time modulated phased array (STMPA) [16] was proposed and good performance was obtained. The harmonic efficiency of STMPA can reach 91.47 %, and its bandwidth of transmission signal can be extended four times. Then an enhanced STMPA (ESTMPA) was proposed in [17], which optimize the design of the I/Q modulator. The harmonic efficiency of ESTMPA reached 94.96% and the transmission signal bandwidth was extended eight times. Recently, the time-pray-phase report technique (TMAPW) was proposed in [18], whose total efficiency can get to 97%, and the signal bandwidth can be extended at a higher multiple. The TMA beamforming system can also use the sum-of-weighted-cosine sequence instead of the RF switches for modulation [19] to improve harmonic efficiency. Thus, a higher harmonic can be used. For example, based on the improved TMA structure, an effective multi-beamforming system enhances the energy of high-order harmonics [20]. All of the above systems effectively improve the efficiency of harmonics.

Although the efficiency of the harmonic beamforming system is improved by changing the system structure, the complexity of its structure becomes higher. An I/Q modulator in STMPA or ESTMPA is connected to one antenna with two channels; thus, when a large number of antenna arrays is required, the system overhead will be much. Therefore, it is necessary to develop a low complexity TMPA harmonic beamforming system. Based on the above proposal and studies [16], [17] by our team, we propose two modified TMPA structures, MSTMPA and ESTMPA, to reduce system complexity and cost.

The paper arranged as follows. Section II introduced the background theory. Here, the concept, structure, and derivation of STMPA and ESTMPA were illustrated and analyzed. Section III presents the proposed systems. The system structure and formula derivation are given. In Section IV, the performance of the proposed system is compared with STMPA and ESTMPA, and their differences and characteristics are discussed in detail. In Section V, the simulation results are given and analyzed to verify the feasibility of the proposed system. Finally, Section VI summarizes the work.

II. BACKGROUND THEORY

An efficient TMA structure STMPA was first proposed in [16], while the ESTMPA [17] (enhanced version of STMPA) was developed later. In this paper, we proposed two improved structures based on these two types, and a brief introduction of the background theory is presented in this section. Fig. 1 shows the basic structure of TMPA, and the STMPA and ESTMPA differ from the I/Q modulator as shown in Fig 2. We introduce the STMPA system in the following subsection.

A. BACKGROUND OF STMPA

Shown in Fig. 2 (a) is the I/Q modulator of STMPA, each antenna is connected to two $0/\pi$ phase shifters and two single-pole single-throw (SPST) switches, whereas one of the paths

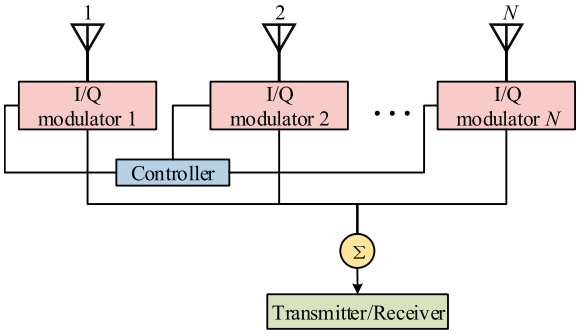

FIGURE 1. The basic structure of traditional TMPA.

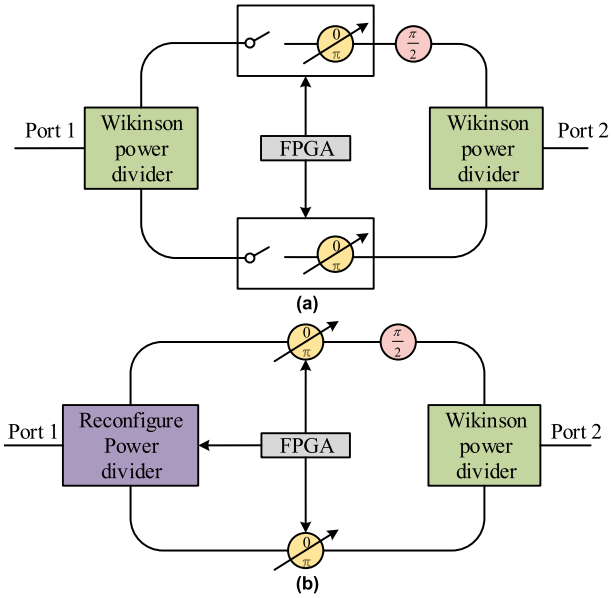

FIGURE 2. The structure of the I/Q modulator in (a) STMPA; (b) ESTMPA.

is connected to a $\pi/2$ fixed-phase shifter. The array factor of an STMPA with N elements can be written as follows

$$AF(\theta, t) = e^{j\omega_0 t} \sum_{n=0}^{N-1} I_n \cdot \left[U_n(t) + jU'_n(t)\right] \cdot e^{jKdn\sin\theta} \quad (1)$$

where $U_n(t)$ and $U'_n(t)$ are two switching functions that turn n-th element either ON or OFF in time, $\omega_0 = 2\pi f_0$ is the angular frequency of the primary signal, $T_p = 1/f_0$ is the modulation period, I_n is the excitation amplitude of the n-th element., K is the wavenumber, and θ is the angle measured from the broad-side direction of the array. (1) can be written as follows

$$AF(\theta, t) = e^{j(\omega_0 + h\omega_p)t} \sum_{n=0}^{N-1} I_n \cdot A_{h,n} \cdot e^{jkdn\sin\theta} \quad (2)$$

where h represents the number of harmonics and $A_{h,n}$ is defined as follows

$$A_{h,n} = a_{h,n} + ja'_{h,n} \quad (3)$$

where $a_{n,h}$ and $a'_{h,n}$ are the Fourier series coefficient of $U_n(t)$ and $U'_n(t)$, respectively.

B. BACKGROUND OF ESTMPA

As shown in Fig. 2 (b) is the structure of the I/Q modulator in ESTMPA, the difference is that ESTMPA uses reconfigure power divider to replace the Wilkinson power divider and canceled the SPST. The array factor of ESTMPA can be written as follows

$$AF(\theta, t) = e^{j(\omega_0 + h\omega_p)t} \sum_{n=0}^{N-1} I_n \cdot A_{h,n}^{+} \cdot e^{jKdn\sin\theta} \tag{4}$$

where $A_{h,n}^{+}$ denotes the equivalent complex excitation.

C. ASSESSMENT

Through hardware structure improvement, STMPA and ESTMPA can suppress most of the harmonics, and the efficiency of TMA is improved. However, they face problems. Because of the single-sideband structure, each I/Q modulator requires two channels, and the complexity and cost of the system will increase when the number of antennas increases.

III. MODIFIED STMPA AND ESTMPA

This subsection presents the modified structures based on STMPA and ESTMPA.

A. MODIFIED STMPA

The I/Q modulator of modified STMPA (MSTMPA) is shown in Fig 3. (b) in the part inside the dotted line, and it is found that each path is connected to an antenna separately. $U_n(t)$ and $U_n'(t)$ denote switch function, while $a_{h,n}$ and $a_{h,n}'$ denote the Fourier series coefficient. $U_n(t)$ and $U_n'(t)$ is written as follows.

$$U_n(t) = \begin{cases} 1, & t_{1n} < t < t_{1n} + \tau \\ -1, & t_{2n} < t < t_{2n} + \tau \\ 0, & else \end{cases} \tag{5}$$

$$U_n'(t) = \begin{cases} 1, & t_{1n}' < t < t_{1n}' + \tau \\ -1, & t_{2n}' < t < t_{2n}' + \tau \\ 0, & else \end{cases} \tag{6}$$

where t_{1n}, t_{2n}, t_{1n}', and t_{2n}' represent the switch-ON duration for 0-state and π-state of two STST switches, respectively.

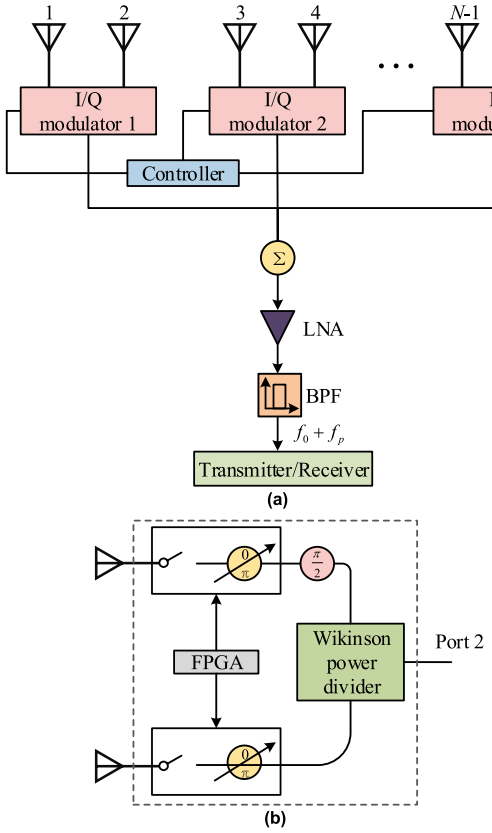

FIGURE 3. (a) The basic structure of modified TMPA; (b) the I/Q modulator of modified STMPA.

τ denotes the duration time, and the relationship between them is shown in Fig. 4.

Assuming that each element is switched in order, then $U_n(t)$ and $U_n'(t)$ can be expressed as follows

$$U_n(t) = \sum_{h=-\infty}^{\infty} a_{h,n} e^{j2\pi cF_p t} dt \tag{7}$$

$$U_n'(t) = \sum_{h=-\infty}^{\infty} a_{h,n}' e^{j2\pi KF_p t} dt \tag{8}$$

where $a_{h,n}$ and $a_{h,n}'$ is defined as (9) and (10) as shown at the bottom of the page.

$$\begin{aligned} a_{h,n} &= \frac{1}{T_p}\int_0^{T_p} U_n(t)\, e^{-jh\omega_p t} dt = \frac{1}{T_p}\left(\int_{t_{1n}}^{t_{1n}+\tau} e^{-jh\omega_p t} dt - \int_{t_{2n}}^{t_{2n}+\tau} e^{-jh\omega_p t} dt\right) \\ &= \begin{cases} \dfrac{2}{h\pi}\sin\left(h\pi\dfrac{\tau}{T_p}\right)\sin\left(h\pi\dfrac{t_{2n}-t_{1n}}{T_p}\right) e^{-j\pi h\frac{t_{2n}+t_{1n}+\tau}{T_p}} e^{j\frac{\pi}{2}}, & if\ h \neq 0, n = 1, \cdots, N \\ 0, & if\ h = 0, n = 1, \cdots, N \end{cases} \end{aligned} \tag{9}$$

$$\begin{aligned} a_{h,n}' &= \frac{1}{T_p}\int_0^{T_p} jU_n'(t)\, e^{-jh\omega_p t} dt = \frac{j}{T_p}\left(-\int_{t_{1n}'}^{t_{1n}'+\tau} e^{-jh\omega_p t} dt + \int_{t_{2n}'}^{t_{2n}'+\tau} e^{-jh\omega_p t} dt\right) \\ &= \begin{cases} \dfrac{2}{h\pi}\sin\left(h\pi\dfrac{\tau}{T_p}\right)\sin\left(h\pi\dfrac{t_{2n}'-t_{1n}'}{T_p}\right) e^{-j\pi h\frac{t_{1n}'+t_{2n}'+\tau}{T_p}}, & if\ h \neq 0, n = 1, \cdots, N \\ 0, & if\ h = 0, n = 1, \cdots, N \end{cases} \end{aligned} \tag{10}$$

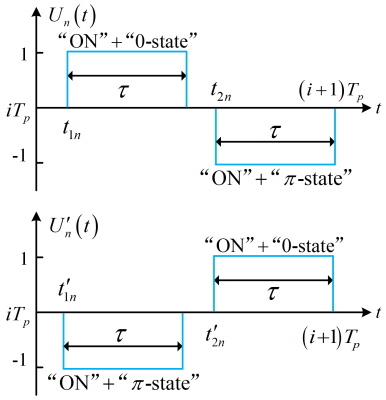

FIGURE 4. The switching sequences of a channel in STMPA.

By observing the term $\sin\left(h\pi\left(t_{2n}-t_{1n}\right)/T_p\right)$ in (9) and (10), it can be seen that even harmonics can be eliminated when (11) is satisfied.

$$\frac{t_{2n}-t_{1n}}{T_p}=\frac{t'_{2n}-t'_{1n}}{T_p}=\frac{1}{2} \tag{11}$$

Further, the term $\sin\left(h\pi\,\tau/T_p\right)$ in (9) and (10) shows that the $3k$-th ($k\in\mathbb{Z}$) harmonics can be eliminated with the following relationship of time (12) as shown at the bottom of the page.

By substituting (11) and (12) to (9) and (10), we can get the equivalent complex excitation as described in (13), as shown at the bottom of the page. Then we can get the equivalent complex excitation of $\pm1^{\text{st}}$ harmonics, as follows

$$A_{+1,n}=\frac{\sqrt{3}}{\pi}\cdot\left\{e^{-j\pi\left(\frac{2t_{1n}}{T_p}+\frac{1}{3}\right)}+e^{-j\pi\left[2\left(\frac{t'_{1n}}{T_p}+\frac{1}{4}\right)+\frac{1}{3}\right]}\right\} \tag{14}$$

$$A_{-1,n}=\frac{\sqrt{3}}{\pi}\cdot\left\{-e^{j\pi\left(\frac{2t_{1n}}{T_p}+\frac{1}{3}\right)}+e^{j\pi\left[2\left(\frac{t'_{1n}}{T_p}+\frac{1}{4}\right)+\frac{1}{3}\right]}\right\} \tag{15}$$

To eliminate the -1^{st} harmonic, (15) should be 0, and the following equation is used to satisfy the above requirement

$$\frac{t'_{1n}}{T_p}=\frac{t_{1n}}{T_p}-\frac{1}{4} \tag{16}$$

Following the relationship of switching time, $A_{h,n}$ can be rewritten as (17), as shown at the bottom of the page, (where sgn $(\cdot)$ is the sign function.). Then the array factor of STMPA can be written as (18), and we can find that the $2k$-th, $3k$-th, and $(4k-1)$-th harmonics ($k\in\mathbb{Z}$) are eliminated.

For beam steering, the relationship between the pointing direction and switching time can be written as follows

$$\frac{t_{1n}}{T_p}=\frac{1}{2}\left[\frac{nKd\sin\theta_d}{\pi}-\frac{1}{3}\right] \tag{19}$$

With (18), the harmonic beamforming of $+1^{\text{st}}$ harmonic can be performed in STMPA.

The objective of MSTMPA is to reduce the complexity of the system while minimizing the magnitude of changes for harmonic beamforming. Fig 3. (a) shows the basic structure of the modified TMPA; it is different from the traditional TMPA in that a channel within each I/Q modulator is connected to a separate antenna, thus improving the utilization of the I/Q modulator. Based on the above discussion, we will give the derivation of MSTMPA.

Based on the idea of simplification, the first step is to increase the utilization of each I/Q modulator. Each channel was initially connected to an antenna, but after improvement, each channel can be connected to an antenna separately. Thus, the array factor of MSTMPA is no longer (18), as shown at the bottom of the page, and the equivalent complex excitation changes. The time term $U_n(t)+jU'_n(t)$ should be separated, and the array factor of MSTMPA can be written as (20) and (21), as shown at the bottom of the next page. Then the structure of MSTMPA can be constructed as shown in Fig. 3 (b).

$$\frac{\tau}{T_p}=\frac{1}{3} \tag{12}$$

$$A_{h,n}=\frac{2}{h\pi}\sin\left(\frac{h\pi}{3}\right)\sin\left(\frac{h\pi}{2}\right)\operatorname{sgn}(h)\left\{e^{-j\pi h\left(\frac{2t_{1n}}{T_p}+\frac{1}{3}\right)}e^{j\pi\frac{1-h}{2}}+e^{-j\pi h\left[2\left(\frac{t'_{1n}}{T_p}+\frac{1}{4}\right)+\frac{1}{3}\right]}\right\} \tag{13}$$

$$A_{h,n}=\begin{cases}\dfrac{2}{h\pi}\sin\left(\dfrac{h\pi}{3}\right)\sin\left(\dfrac{h\pi}{2}\right)\operatorname{sgn}(h)\,e^{-j\pi h\left(\frac{2t_{1n}}{T_p}+\frac{1}{3}\right)}\left(e^{j\pi\frac{1-h}{2}}+1\right), & \text{if } h\neq0, n=1,\cdots,N\\ 0, & \text{if } h=0, n=1,\cdots,N\end{cases} \tag{17}$$

$$AF_h(\theta)=\begin{cases}\displaystyle\sum_{n=0}^{N-1}\frac{2\sqrt{3}}{\pi}I_n e^{-j\pi\left(\frac{2t_{1n}}{T_p}+\frac{1}{3}\right)}e^{jKdn\sin\theta}, & \text{if } h=1\\ 0, & \text{if } h=2k\cup3k\cup4k-1, k\in\mathbb{Z}\\ \displaystyle\sum_{n=0}^{N-1}\frac{4}{3}\sin c\left(\frac{h\pi}{3}\right)\operatorname{sgn}(h)\,I_n e^{-jh\pi\left(\frac{2t_{1n}}{T_p}+\frac{1}{3}\right)}e^{jKdn\sin\theta}, & \textit{others}\end{cases} \tag{18}$$

Observing (21), we can find that the $2k$-th, $3k$-th, harmonic ($k \in \mathbb{Z}$) can still be eliminated with the switching sequence of STMPA, but the $4k-1$-th harmonics cannot. It is because two paths are connected to an antenna separately, and the equivalent complex excitations $A_{h,n}$ are not suitable for this case. As written in (22), as shown at the bottom of the page, $a_{h,n}$ and $ja'_{h,n}$ are separately times a phase term. Here, an additional phased term is added $ja'_{h,n}$. Based on the above analysis, we can remove the $\pi/2$ fixed-phase shifter to further simplify the system, as shown in Fig. 5 (a). Then the term $e^{j\pi\frac{1-h}{2}}$ in (18) is omitted, and the array factor of MSTMPA can be written as (22). Besides, the term $e^{jKd\sin\theta}$ in (22) should be considered.

As the $\pi/2$ fixed-phase shifter is removed, the relationship (16) can be ignored. The new relation of t_{1n} and t'_{1n} can be used to deal with the additional phase term, which can be written as follows (23), as shown at the bottom of the page.

$$\frac{t'_{1n}}{T_p} = \frac{t_{1n+1}}{T_p} \tag{24}$$

Then the additional phase term $e^{jKd\sin\theta}$ can be eliminated, and the array aperture is doubled. Finally, the array factor of MSTMPA can be rewritten as (24).

Compared to the traditional STMPA, the MSTMPA has reduced the system cost, but the $4k-1\cap 3k$-th harmonics cannot be eliminated due to the modified structure. Hence, a bandpass filter (BPF) is used to extract the $+1^{\text{st}}$ harmonic, as shown in Fig. 3 (a). Accordingly, the harmonic efficiency will decrease, but the efficiency of the feeding network efficiency will increase. We will elaborate on the specific analysis of the efficiency in the next section.

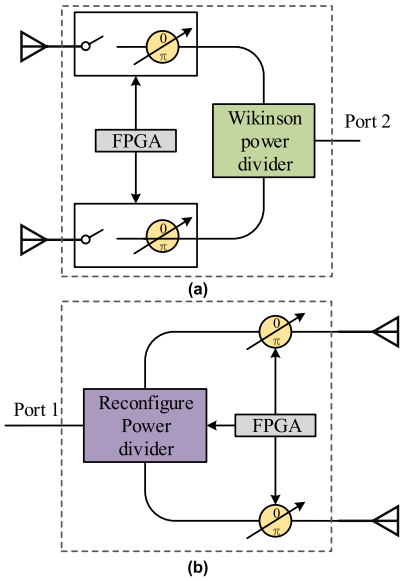

FIGURE 5. (a) The I/Q modulator of modified STMPA (version II); (b) the I/Q modulator of modified ESTMPA.

B. MODIFIED ESTMPA

Considering that ESTMPA has better performance than STMPA and that we can modify it to MESTMPA. The switching sequences of ESTMPA are shown in Fig. 6. Several principles of switching time are the same as STMPA

$$AF(\theta,t) = e^{j\omega_0 t}\sum_{n=0}^{N-1}\left[U_n(t)\,e^{jKd2n\sin\theta} + jU'_n(t)\,e^{jKd(2n+1)\sin\theta}\right] = e^{j(\omega_0+h\omega_p)t}\sum_{n=0}^{N-1}\left[a_{h,n}e^{jKd2n\sin\theta} + ja'_{h,n}e^{jKd(2n+1)\sin\theta}\right] \tag{20}$$

$$AF(\theta,t) = e^{j(\omega_0+h\omega_p)t}\frac{2}{h\pi}\sin\left(\frac{h\pi}{3}\right)\sin\left(\frac{h\pi}{2}\right)\mathrm{sgn}(h)\sum_{n=0}^{N-1}e^{-jh\pi\left(\frac{2t_{1n}}{T_p}+\frac{1}{3}\right)}\left[e^{j\pi\frac{1-h}{2}}e^{jKd2n\sin\theta} + e^{jKd(2n+1)\sin\theta}\right] \tag{21}$$

$$\begin{aligned} AF(\theta,t) &= e^{j\omega_0 t}\sum_{n=0}^{N-1}\left[U_n(t)\,e^{jKd2n\sin\theta} + U'_n(t)\,e^{jKd(2n+1)\sin\theta}\right] = e^{j(\omega_0+h\omega_p)t}\sum_{n=0}^{N-1}\left[a_{h,n}e^{jKd2n\sin\theta} + a'_{h,n}e^{jKd(2n+1)\sin\theta}\right] \\ &= e^{j(\omega_0+h\omega_p)t}\frac{2}{h\pi}\sin\left(\frac{h\pi}{3}\right)\sin\left(\frac{h\pi}{2}\right)\mathrm{sgn}(h)\sum_{n=0}^{N-1}\left[e^{jKd2n\sin\theta-jh\pi\left(\frac{2t_{1n}}{T_p}+\frac{1}{3}\right)} + e^{jKd2n\sin\theta-jh\pi\left(\frac{2t'_{1n}}{T_p}+\frac{1}{3}\right)}e^{jKdn\sin\theta}\right] \end{aligned} \tag{22}$$

$$AF_m = \begin{cases} \sum_{n=0}^{2N-1}\frac{\sqrt{3}}{\pi}e^{-j\pi h\left(\frac{2t_{1n}}{T_p}+\frac{1}{3}\right)}e^{jKdn\sin\theta}, & h=(4k\pm1)\cap 3k, k\in\mathbb{Z} \\ 0, & h=2k\cup 3k, k\in\mathbb{Z} \\ \frac{4}{3}\sin c\left(\frac{h\pi}{3}\right)\mathrm{sgn}(h)\sum_{n=0}^{2N-1}e^{-j\pi h\left(\frac{2t_{1n}}{T_p}+\frac{1}{3}\right)}e^{jKdn\sin\theta}, & others \end{cases} \tag{23}$$

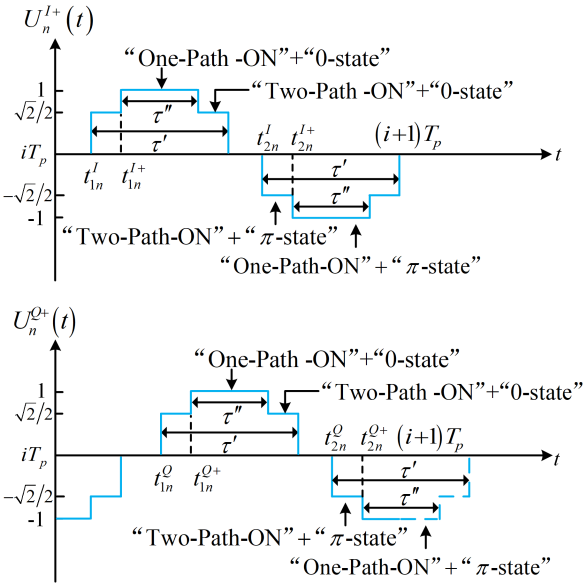

FIGURE 6. The switching sequences of a channel in ESTMPA.

as follows

$$\frac{t_{2n}^{Q}-t_{1n}^{Q}}{T_p}=\frac{t_{2n}^{I}-t_{1n}^{I}}{T_p}=\frac{1}{2} \tag{25}$$

$$\frac{t_{1n}^{I}}{T_p}=\frac{t_{1n}^{Q}}{T_p}-\frac{1}{4} \tag{26}$$

Some principles different from STMPA are created to enhance harmonic suppression. First, is the one-path state, shown in Fig. 6. The relation of duration time should satisfy the following equation

$$\frac{t_{1n}^{I+}-t_{1n}^{I}}{T_p}=\frac{t_{2n}^{I+}-t_{2n}^{I}}{T_p}=\frac{t_{1n}^{Q+}-t_{1n}^{Q}}{T_p}=\frac{t_{2n}^{Q+}-t_{2n}^{Q}}{T_p}=\frac{\tau'-\tau''}{2T_p} \tag{27}$$

where t_{1n}^{I+}, t_{2n}^{I+}, t_{1n}^{Q+}, and t_{2n}^{Q+} represent the one-path switch-ON state starting instants, t_{1n}^{I}, t_{1n}^{Q}, t_{2n}^{I}, and t_{2n}^{Q} represent the two-path switch- ON state starting instants and the others are similar to those of STMPA. In the one-path state, the transfer of powers into one channel turns off another channel. In the two-path state, the power is equally divided and transferred into two channels. The two states form the stepped waveforms, which is different from the switching sequences in STMPA. Then the equivalent complex excitations $A_{h,n}^{+}$ of ESTMPA are expressed as (28), shown at the bottom of the page.

It can be found from (28) that ESTMPA could eliminate more undesired harmonics ($h=8k+4\pm1$, $k\in\mathbb{Z}$) than STMPA if theses equations are satisfied

$$\frac{\tau'}{T_p}=\frac{3}{8},\frac{\tau''}{T_p}=\frac{1}{8} \tag{29}$$

$A_{h,n}^{+}$ can be rewritten as (30), shown at the bottom of the page, and the harmonic efficiency is improved from 91.19% (STMPA) to 94.46%. Now let us discuss the design of MESTMPA. From the analysis in the previous section, the $\pi/2$ fixed-phase shifter can be removed in MESTMPA. Besides, the relation like (24) in MSTMPA should also be considered in MESTMPA to eliminate the additional phase term, which can be written as follows

$$\frac{t_{1n}^{Q}}{T_p}=\frac{t_{1n+1}^{I}}{T_p},\frac{t_{1n}^{Q+}}{T_p}=\frac{t_{1n+1}^{I+}}{T_p},\frac{t_{2n}^{Q}}{T_p}=\frac{t_{2n+1}^{I}}{T_p},\frac{t_{2n}^{Q+}}{T_p}=\frac{t_{2n+1}^{I+}}{T_p} \tag{31}$$

In addition, we should change the order of the input and output signals. Because the reconfigurable power divider functions like the SPST switch in STMPA, port 2 is modified, and port 1 exports the modulated signal. Then, the equivalent complex excitations of MESTMPA can be rewritten as (32), shown at the bottom of the next page, and the array factor can be expressed as (33), shown at the bottom of the next page. It can be found from (33) that the MESTMPA does not eliminate the $8k-1$-th harmonics; thus, the BPF is also needed. The structure of MESTMPA is shown in Fig. 5 (b).

In this section, we have introduced the design of two modified structures, and more on harmonic suppression will be discussed in the next section.

IV. PERFORMANCE COMPARSION

This section discusses the performance of the proposed systems. There are three points of evaluation, one is harmonic suppression, one is efficiency, and the other is the radiation pattern.

A. HARMONIC SUPPRESSION

The first to discuss is the performance of harmonic suppression. Suppose the incident direction is set as 90°, then the power spectra of the proposed systems, STMPA, and ESTMPA are shown in Fig. 7 (a) and (b). It can be found

$$A_{h,n}^{+}=\begin{cases}\dfrac{1}{|h|\,\pi}\left[\sin\left(\dfrac{h\pi\,\tau'}{T_p}\right)+\left(\sqrt{2}-1\right)\sin\left(\dfrac{h\pi\,\tau''}{T_p}\right)\right]\sin\left(\dfrac{h\pi}{2}\right)\left(e^{j\pi\frac{1-h}{2}}+1\right)e^{-jh\pi\left(2t_{1n}^{I}+\frac{1}{3}\right)}, & h\neq 0\\ 0, & others\end{cases} \tag{28}$$

$$A_{h,n}^{+}=\begin{cases}\dfrac{2}{|h|\,\pi}\left[\sin\left(\dfrac{3\pi}{8}\right)+\left(\sqrt{2}-1\right)\sin\left(\dfrac{\pi}{8}\right)\right]e^{-jh\pi\left(2t_{1n}^{I}+\frac{1}{3}\right)}, & \text{if } h=8k+1,k\in\mathbb{Z}\\ 0, & others\end{cases} \tag{30}$$

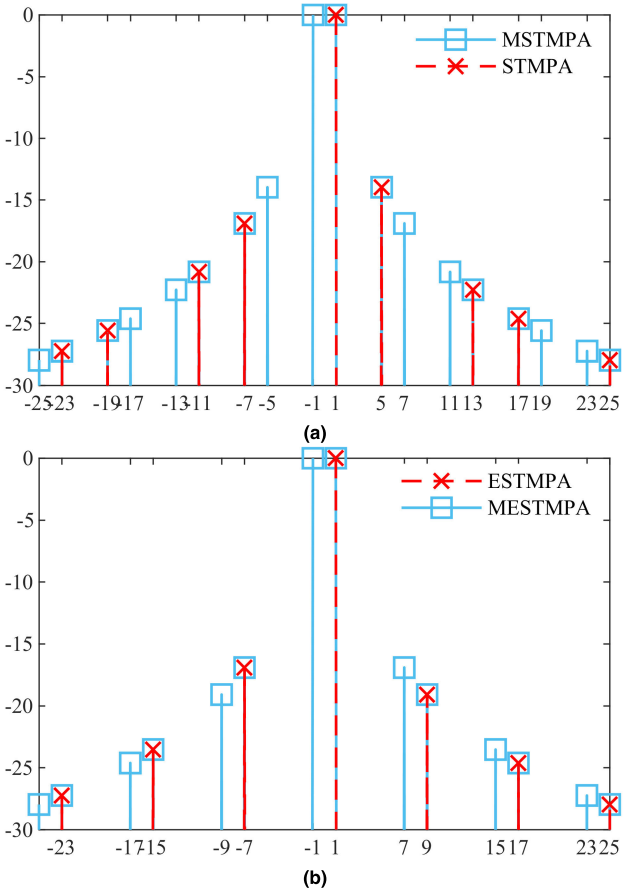

FIGURE 7. Normalized power spectrums for (a) MSTMPA and STMPA; (b) MESTMPA and ESTMPA.

that the SBL of the proposed systems is the same before their modification, but the undesired harmonics are increased. Fig. 7 (a) shows that the $4k-1 \cap 3k$-th harmonics cannot be eliminated in MSTMPA and Fig. 7 (b) shows that the $8k-1$-th harmonics cannot be eliminated in MESTMPA. This result is because the single sideband structure has removed from the original structure. Due to the use of BPF, the harmonic beamforming based on $+1^{\text{st}}$ harmonic will not be affected.

B. EFFICIENCY

Compared with STMPA and ESTMPA, the efficiency of the two proposed systems is discussed in this subsection. As described in [17], the efficiency of TMA η^T including the

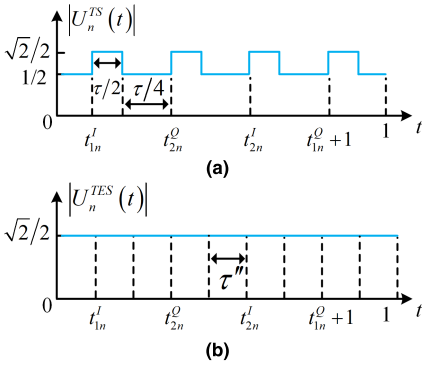

FIGURE 8. The modulating waveforms of the *n* -th I/Q modulator in (a) STMPA; (b) ESTMPA.

feeding network efficiency η^F and harmonic efficiency η^H. η^T is expressed as follows

$$\eta^T = \eta^H \cdot \eta^F \tag{34}$$

As a matter of fact, since there is no perfect cancelation in practice, undesired harmonics will not all be suppressed; thus, filters are still needed. Therefore, the harmonic efficiency of the system remains unchanged, and we should focus on the feeding network efficiency of the system. The feeding network efficiency of the system shown in the expression below

$$\eta^H = 1/T_P \cdot \int_0^{T_p} |U(t)|^2 \, dt \tag{35}$$

From (32), it can be found that the feeding network efficiency is decided by the modulating waveform of the I/Q modulator. The modulating waveform in STMPA and ESTMPA is shown in Fig. 8 (a) and (b). However, although the modulating waveform in MSTMPA and MESTMPA is the same in each channel in STMPA and ESTMPA (as shown in Fig. 4 and Fig. 6, each channel is separately connected to an antenna in a modified I/Q modulator. Thus, the feeding network efficiency will be changed.

η^F of MSTMPA can be calculated as follows

$$\begin{aligned} &\eta^H_{MSTMPA} \\ &= 1/T_P \cdot \left(\int_{t_{1n}}^{t_{1n}+\tau} |U(t)|^2 \, dt + \int_{t_{2n}}^{t_{2n}+\tau} |U(t)|^2 \, dt \right) \\ &= 1/T_P \cdot 2\tau = 2/3 \end{aligned} \tag{36}$$

$$A^+_{h,n} = \begin{cases} \dfrac{2}{|h|\,\pi} \displaystyle\sum_{n=0}^{N-1} \left[\sin\left(\frac{3\pi}{8}\right) + \left(\sqrt{2}-1\right) \sin\left(\frac{\pi}{8}\right) \right] e^{-jh\pi\left(2t^I_{1n}+\frac{1}{3}\right)}, & \text{if } h = 8k \pm 1, k \in \mathbb{Z} \\ 0, & \text{others} \end{cases} \tag{32}$$

$$AF(\theta, t) = \begin{cases} e^{j(\omega_0 + h\omega_p)t} \displaystyle\sum_{n=0}^{2N-1} \frac{2}{|h|\,\pi} \left[\sin\left(\frac{3\pi}{8}\right) + \left(\sqrt{2}-1\right) \sin\left(\frac{\pi}{8}\right) \right] e^{-j\pi\left(2t^I_{1n}+\frac{1}{3}\right)} e^{jKdn\sin\theta}, & \text{if } h = 8k \pm 1, k \in \mathbb{Z} \\ 0, & \text{others} \end{cases} \tag{33}$$

TABLE 1. Comparison of efficiency of different kinds of TMPAs.

	Feeding network efficiency
MSTMPA	66.67%
STMPA	33.33%
MESTMPA	50%
ESTMPA	50%

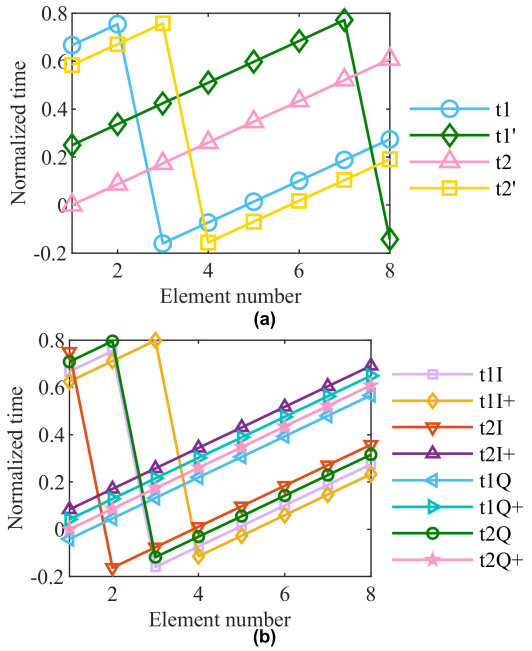

FIGURE 9. Normalized switch time of incident direction 10° for (a) STMPA; (b) ESTMPA.

η^F of MESTMPA can be calculated as follows

$$\eta^H_{MESTMPA} = 1/T_P \cdot \begin{pmatrix} \int_{t^I_{1n}}^{t^{I+}_{1n}} 1/2dt + \int_{t^{I+}_{1n}}^{t^{I+}_{1n}+\tau''} dt + \int_{t^{I+}_{1n}+\tau''}^{t^{I}_{1n}+\tau'} 1/2dt \\ + \int_{t^{I}_{2n}}^{t^{I+}_{2n}} 1/2dt + \int_{t^{I+}_{2n}}^{t^{I+}_{2n}+\tau''} dt + \int_{t^{I+}_{2n}+\tau''}^{t^{I}_{2n}+\tau'} 1/2dt \end{pmatrix}$$
$$= 1/T_P \cdot 2\left[(\tau'' + \tau')/2\right] = 1/2 \quad (37)$$

The feeding network efficiency of different kinds of TMPA is given in table 1. It can be seen that the feeding network efficiency of MSTMPA is doubled, while that of MESTMPA remains unchanged. The modified I/Q modulator did not cause the loss of switching time.

C. RADIATION PATTERN

As the modified I/Q modulators are each connected to antennas, the space between each antenna should be set as half the wavelength to avoid the grating lobe; thus, the array aperture will be doubled using the modified I/Q modulator and better performance will be obtained. This section will verify it using numerical simulations.

V. NUMERICAL SIMULATIONS

This section gives several examples of the proposed system to verify the derivations and equations.

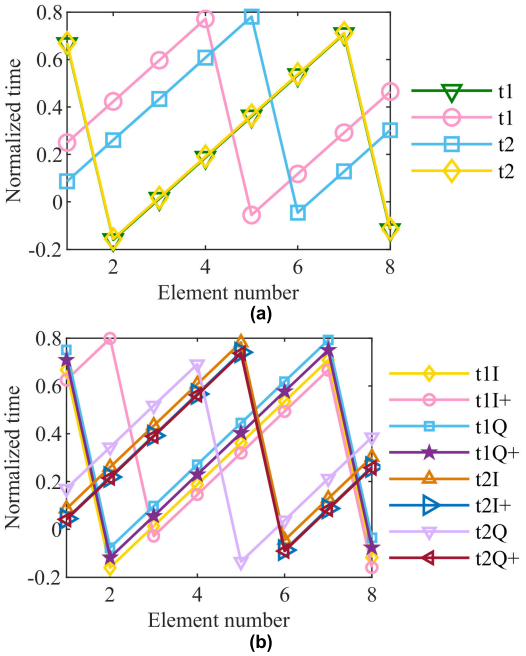

FIGURE 10. Normalized switch time of incident direction 10° (a) MSTMPA; (b) MESTMPA.

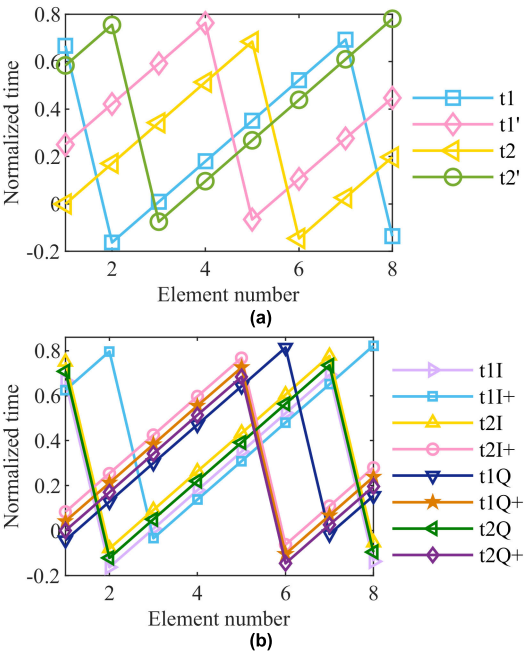

FIGURE 11. Normalized switch time of incident direction 20° for (a) STMPA; (b) ESTMPA.

The proposed systems are compared with STMPA and ESTMPA. The number of I/Q modulators is set as eight for each type of array (STMPA, ESTMPA, MSTMPA, and MESTMPA), and the static amplitudes are all set as one. The main frequency of the signal is $f_0 = 5$ GHz and the switching frequency is set as $F_p = 100$ KHz. Besides, the element spacing is set as $d = \lambda/2$ for all mentioned systems.

Suppose the pointing direction of the beam is set as 10° and 20° for testing the performance of different kinds of arrays.

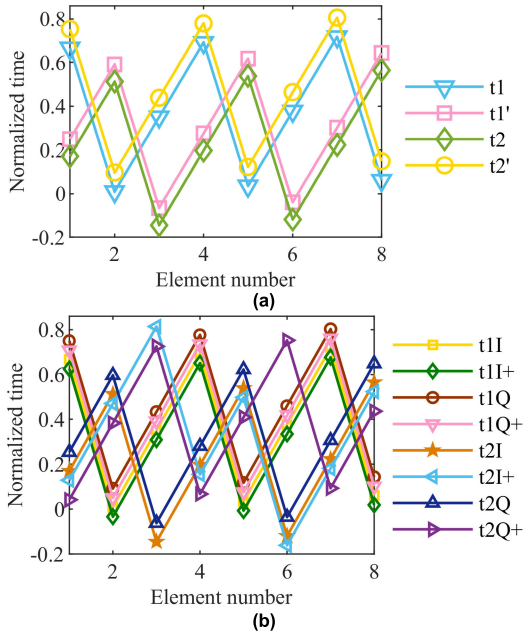

FIGURE 12. Normalized switch time of incident direction 20° (a) MSTMPA; (b) MESTMPA.

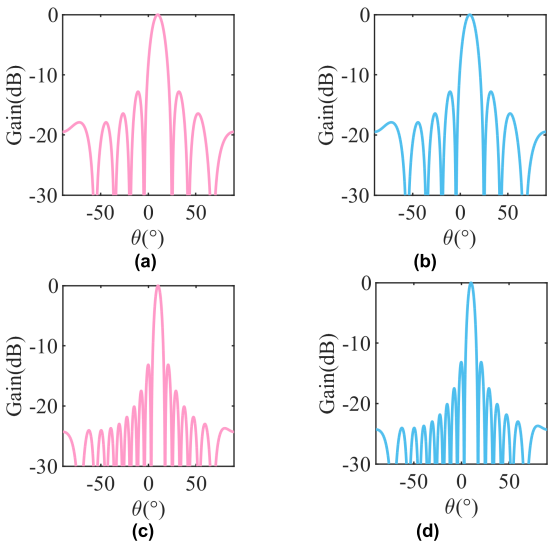

FIGURE 13. The radiation pattern in direction of 10° by (a) STMPA; (b) ESTMPA; (c) MSTMPA; (d) MESTMPA.

The switching sequences for different arrays are shown in Fig. 9, Fig 10, Fig 11, and Fig 12. Because using BPF, the generated beam only left the $+1^{st}$ harmonic. The simulated radiation pattern of STMPA and ESTMPA is shown in Fig. 13 (a), (b) and Fig 14 (a), (b), and it can be found that the beam is formed as desired. Fig. 13 (c), (d), and Fig 14 (c), (d) shows the generated radiation pattern of MSTMPA and MESTMPA. We can find that the beamwidth of MSTMPA and MESTMPA is smaller than that of STMPA and ESTMPA. The performance of different kinds of arrays is summarized in Table 2. We can find that the beamwidth of the proposed systems is narrower and the sidelobe level is lower than that of STMPA and ESTMPA.

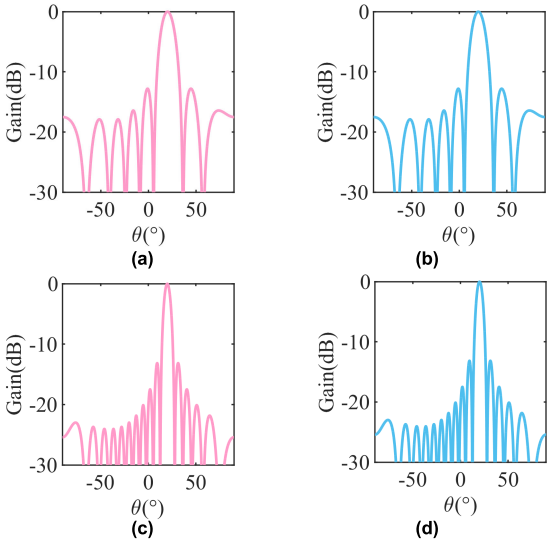

FIGURE 14. The radiation pattern in direction of 20° by (a) STMPA; (b) ESTMPA; (c) MSTMPA; (d) MESTMPA.

TABLE 2. Comparison of radiation pattern of TMPAs.

	Incident direction (°)	Beamwidth (°)	Sidelobe level (dB)
MSTMPA	10	6.42	−13.15
STMPA	10	13.1	−12.80
MESTMPA	10	6.48	−13.15
ESTMPA	10	13.08	−12.80
MSTMPA	20	6.82	−13.15
STMPA	20	13.9	−12.80
MESTMPA	20	6.8	−13.15
ESTMPA	20	13.9	−12.80

VI. CONCLUSION

In this study, the modified STMPA and ESTMPA are proposed. The derivations are presented and the principle of the proposed systems are compared with STMPA and ESTMPA. Unlike their structure, the proposed system modifies the I/Q modulator to separate the two signals that were initially connected and connect them to a separate antenna. The proposed systems show less complexity and thus have lower hardware overhead. In addition, the array aperture will be enlarged with the same number of I/Q modulators, and better pattern performance can be obtained. However, these changes the original single sideband structure, hence, the proposed systems cannot eliminate a series of harmonics represented by the -1^{st} harmonics. Due to the use of BPF at the output, the impact of these extra harmonics is limited.

Meanwhile, the efficiency of the system has changed. For MSTMPA, the efficiency of the feeding network is doubled. For MESTMPA, the efficiency of the feeding network remains unchanged. The efficiency of the harmonics will be slightly reduced because fewer harmonics are eliminated. Therefore, the proposed system simplifies the structure but reduces some harmonic efficiency, which can be considered a compromise. In the future, efficiency will be an important aspect of further investigation.

ACKNOWLEDGMENT

The authors would like to thank the editors and reviewers for their efforts.

REFERENCES

[1] H. E. Shanks and R. W. Bickmore, "Four-dimensional electromagnetic radiators," *Can. J. Phys.*, vol. 37, no. 3, pp. 263–275, Mar. 1959.
[2] S. Yang, Y. B. Gan, and A. Qing, "Sideband suppression in time-modulated linear arrays by the differential evolution algorithm," *IEEE Antennas Wireless Propag. Lett.*, vol. 1, no. 1, pp. 173–175, Jul. 2002.
[3] L. Poli, P. Rocca, L. Manica, and A. Massa, "Time modulated planar arrays—Analysis and optimisation of the sideband radiations," *IET Microw., Antennas Propag.*, vol. 4, no. 9, pp. 1165–1171, Sep. 2010.
[4] Q. Zhu, S. Yang, L. Zheng, and Z. Nie, "Design of a low sidelobe time modulated linear array with uniform amplitude and sub-sectional optimized time steps," *IEEE Trans. Antennas Propag.*, vol. 60, no. 9, pp. 4436–4439, Sep. 2012.
[5] J. Euziere, R. Guinvarc'h, B. Uguen, and R. Gillard, "Optimization of sparse time-modulated array by genetic algorithm for radar applications," *IEEE Antennas Wireless Propag. Lett.*, vol. 13, pp. 161–164, 2014.
[6] Y. Ma, C. Miao, Y. Li, and W. Wu, "Time-modulated sparse linear array synthesis with minimum elements and a specific sidelobe," *IET Microw., Antennas Propag.*, vol. 14, no. 13, pp. 1595–1598, Oct. 2020.
[7] Y. Tong and A. Tennant, "Simultaneous control of sidelobe level and harmonic beam steering in time-modulated linear arrays," *Electron. Lett.*, vol. 46, no. 3, pp. 201–202, Feb. 2010.
[8] L. Poli, P. Rocca, G. Oliveri, and A. Massa, "Harmonic beamforming in time-modulated linear arrays," *IEEE Trans. Antennas Propag.*, vol. 59, no. 7, pp. 2538–2545, Jul. 2011.
[9] Y. Tong and A. Tennant, "A two-channel time modulated linear array with adaptive beamforming," *IEEE Trans. Antennas Propag.*, vol. 60, no. 1, pp. 141–147, Jan. 2012.
[10] C. He, X. Liang, Z. Li, J. Geng, and R. Jin, "Direction finding by time-modulated array with harmonic characteristic analysis," *IEEE Antennas Wireless Propag. Lett.*, vol. 14, pp. 642–645, 2015.
[11] A. Tennant and B. Chambers, "A two-element time-modulated array with direction-finding properties," *IEEE Antennas Wireless Propag. Lett.*, vol. 6, pp. 64–65, 2007.
[12] G. Li, S. Yang, and Z. Nie, "Direction of arrival estimation in time modulated linear arrays with unidirectional phase center motion," *IEEE Trans. Antennas Propag.*, vol. 58, no. 4, pp. 1105–1111, Apr. 2010.
[13] C. Shan, Y. Ma, H. Zhao, and J. Shi, "Joint radar-communications design based on time modulated array," *Digit. Signal Process.*, vol. 82, pp. 43–53, Nov. 2018.
[14] C. He, Q. Chen, A. Cao, J. Chen, and R. Jin, "Application of the time modulated array in satellite communications," *IEEE Wireless Commun.*, vol. 26, no. 2, pp. 24–30, Apr. 2019.
[15] D. Ni, S. Yang, Y. Chen, and J. Guo, "A study on the application of sub-arrayed time-modulated arrays to MIMO radar," *IEEE Antennas Wireless Propag. Lett.*, vol. 16, pp. 1171–1174, 2017.
[16] A.-M. Yao, W. Wu, and D.-G. Fang, "Single-sideband time-modulated phased array," *IEEE Trans. Antennas Propag.*, vol. 63, no. 5, pp. 1957–1968, May 2015.
[17] Q. Chen, J.-D. Zhang, W. Wu, and D.-G. Fang, "Enhanced single-sideband time-modulated phased array with lower sideband level and loss," *IEEE Trans. Antennas Propag.*, vol. 68, no. 1, pp. 275–286, Jan. 2020.
[18] H. Li, Y. Chen, and S. Yang, "Harmonic beamforming in antenna array with time-modulated amplitude-phase weighting technique," *IEEE Trans. Antennas Propag.*, vol. 67, no. 10, pp. 6461–6472, Oct. 2019.
[19] R. Maneiro-Catoira, J. C. Brégains, J. A. García-Naya, and L. Castedo, "Enhanced time-modulated arrays for harmonic beamforming," *IEEE J. Sel. Topics Signal Process.*, vol. 11, no. 2, pp. 259–270, Mar. 2017.
[20] R. Maneiro-Catoira, J. Brégains, J. A. García-Naya, and L. Castedo, "Time-modulated multibeam phased arrays with periodic Nyquist pulses," *IEEE Antennas Wireless Propag. Lett.*, vol. 17, no. 12, pp. 2508–2512, Dec. 2018.

YUE MA (Student Member, IEEE) was born in Jiangsu, China, in 1995. He received the B.E. degree in communication engineering from the Jiangsu University of Technology, Changzhou, China, in 2017. He is currently pursuing the Ph.D. degree in information and communication engineering with the Nanjing University of Science and Technology, Nanjing, China. His research interests include time-modulated array, radar signal processing, and array signal processing. He has been a Reviewer for the *IET Signal processing*.

CHEN MIAO (Member, IEEE) was born in Jiangsu, China, in 1978. He received the B.S., M.S., and Ph.D. degrees in electronic engineering from the Nanjing University of Science and Technology, Nanjing, China, in 2001, 2004, and 2014, respectively. He is currently a Professor with the School of Electronic Engineering and Optoelectronic Technology, Nanjing University of Science and Technology. His research interests include signal processing, microwave and millimeter-wave circuits, and detection technology.

YUE-HUA LI (Member, IEEE) was born in Jiangsu, China, in 1959. He received the B.S., M.S., and Ph.D. degrees in electronic engineering from the Nanjing University of Science and Technology, Nanjing, China, in 1982, 1989, and 1999, respectively. He is currently a Professor with the School of Electronic Engineering and Optoelectronic Technology, Nanjing University of Science and Technology. His research interests include target recognition, signal processing, and detection technology.

WEN WU (Senior Member, IEEE) received the Ph.D. degree in electromagnetic field and microwave technology from Southeast University, Nanjing, China, in 1997. He is currently a Professor with the School of Electronic Engineering and Optoelectronic Technology, Nanjing University of Science and Technology, where he is also the Associate Director with the Ministerial Key Laboratory of JGMT. He has authored or coauthored over 300 journal and conference papers and has submitted over 30 patent applications. His current research interests include microwave and millimeter-wave theories and technologies, microwave and millimeter-wave detection, and multimode compound detection. He was a recipient of the Ministerial and Provincial-Level Science and Technology Awards for six times.